BMC Nephrology

RESEARCH Open Access

Exacerbation of diabetes due to *F. Nucleatum* LPS-induced SGLT2 overexpression in the renal proximal tubular epithelial cells

Aiko Seki[1], Koichiro Kajiwara[2], Jumpei Teramachi[3], Masahiko Egusa[4], Takuya Miyawaki[4] and Yoshihiko Sawa[3*]

Abstract

Background Diabetes treatments by the control of sodium-glucose cotransporter 2 (SGLT2) is commonly conducted while there are still uncertainties about the mechanisms for the SGLT2 overexpression in kidneys with diabetes. Previously, we have reported that glomeruli and proximal tubules with diabetic nephropathy express toll-like receptor TLR2/4, and that the TLR ligand lipopolysaccharide (LPS) of periodontal pathogens have caused nephropathy in diabetic model mice. Recently, many researchers suggested that the periodontal pathogenic bacteria Fusobacterium (F.) nucleatum has the TLR4-associated strong activator of the colorectal inflammation and cancer. The present study aimed to investigate the possibility of F. nucleatum as an exacerbation factor of diabetes through the renal SGLT2 induction.

Methods The induction of the SGLT2 by F. nucleatum LPS (Fn-LPS) were investigated in the streptozotocin-induced diabetic mouse renal tissue and cultured renal proximal epithelial cells. The changes of blood glucose levels and survival curves in diabetic mice with Fn-LPS were analyzed. The Fn-LPS-induced SGLT2 production in the diabetic mouse renal tissue and in the cultured proximal epithelial cells was examined by ELISA, quantitative RT-PCR, and immunohistochemical analysis.

Results The SGLT2 expression in the cultured mouse tubular epithelial cells was significantly increased by TNF- or co-culture with Fn-LPS-supplemented J774.1 cells. The period to reach diabetic condition was significantly shorter in Fn-LPS-administered diabetic mice than in diabetic mice. All Fn-LPS-administered-diabetic mice reached humane endpoints during the healthy period of all of the mice administered Fn-LPS only. The promotion of the SGLT2 expression at the inner lumen of proximal tubules were stronger in the Fn-LPS-administered-diabetic mice than in diabetic mice. The renal tissue SGLT2 mRNA amounts and the number of renal proximal tubules with overexpressed SGLT2 in the lumen were more in the Fn-LPS-administered-diabetic mice than in diabetic mice.

Conclusions This study suggests that F. nucleatum causes the promotion of diabetes through the overexpression of SGLT2 in proximal tubules under the diabetic condition. Periodontitis with F. nucleatum may be a diabetic exacerbating factor.

Keywords *F. Nucleatum*, Diabetic exacerbation, Diabetic nephropathy, SGLT2

*Correspondence:
Yoshihiko Sawa
ysawa@okayama-u.ac.jp

Full list of author information is available at the end of the article

Introduction

Exacerbation of diabetes may be fatal due to complications such as diabetic nephropathy caused by chronic inflammatory glomerulosclerosis [1, 2]. It has been discussed that periodontal diseases may contribute to diabetic complications and the exacerbation of diabetes, but there are many unclear aspects related to the interaction between diabetes and periodontal diseases [3–7]. In addition, sodium-glucose cotransporter 2 (SGLT2) is responsible for glucose reabsorption in the proximal renal tubules and SGLT2 inhibitors have attracted attention for diabetes control [8, 9], but the renal SGLT2 increase system in the tubules under diabetic circumstances has not also been fully elucidated [10–13]. Recently, we reported that glomerular endothelial cells in diabetic kidneys express toll-like receptor TLR2/4 but are not expressed in the surrounding renal small blood vessels [14–16]. The TLRs are innate immune receptors sensing pathogen-associated molecular patterns and play a role in innate immunity [17–19]. The TLR2/4 are commonly expressed on phagocytes and the recognition of lipoteichoic acid from Gram-positive bacteria and lipopolysaccharide (LPS) from Gram-negative bacteria by TLR2/4 induces the production of inflammatory cytokines. Since the excessive signal transduction via TLR2/4 induces a cytokine storm like SARS-CoV-2 pneumonia, TLR2/4 expression is usually not observed in blood vessels in general tissues [14–19]. In a hyperglycemic environment advanced glycation end products (AGEs) are generated by non-catalytic glucose modification of the blood proteins, accumulate in organs with complex structures like renal glomeruli, stimulate leukocytes and cause the TLR2/4 expression in the glomerular endothelial cells by the chronic activation via the interaction of AGEs and receptor for AGEs (RAGE), which is ubiquitously expressed in somatic cells [1, 2, 20–27]. Elevated levels of TLR2/4 expression have been reported in leukocytes and kidney in diabetic patients and animal models. It has been thought that hyperglycemia induces the TLR2/4 expression in leukocytes and that AGEs are recognized by leukocytes via TLR2/4 in the renal tissue. The recognition of AGEs in the renal TLR has been suggested as one candidate promoting tubular inflammation and interstitial fibrosis in diabetic nephropathy [21–32]. Furthermore, it is speculated that the inflammatory response via TLR in renal tissue and leukocytes in the presence of periodontal pathogens in the renal microcirculation induces the production of inflammatory cytokines which promote inflammatory events in kidneys [24–30].

In our recent studies, we have reported that the administration of *Porphyromonas (P). gingivalis* LPS under the buccal mucosa caused the nephropathy in the streptozotocin (STZ)-induced diabetic mice as an infection model for the oral circulatory invasion of periodontal pathogens [14, 15]. In these studies all of the *P. gingivalis* LPS-administered diabetic mice reached humane endpoints with nephropathy within the survival period of all of the diabetic mice and LPS-administered healthy mice, and that the TLR4 inhibitor eritoran suppresses nephropathy [16]. Since *P. gingivalis* LPS is a TLR2-dominant ligand with weak activation to TLR4, it was speculated that even a weak level of TLR4 activation would cause an inflammatory response in diabetic kidneys. Therefore, we further investigated the inflammatory events in the kidney of *P. gingivalis* LPS-administered diabetic mice and found that *P. gingivalis* LPS caused the abnormal renal tubular expression of the leukocyte adhesion molecule; vascular endothelial cell adhesion molecule-1 (VCAM-1), and the overexpression of SGLT2 [33, 34]. Bacteria causing oral infections such as periodontal diseases directly enter the systemic circulation, spread throughout the body, and reach a number of organs [4–6]. For the example, it is well known that streptococci-IgA-immune complexes which have formed in the tonsils accumulate in the glomeruli and cause IgA nephropathy [3–6]. On the contrary, intestinal bacteria that enter the intestinal circulation do not cause sepsis because intestinal bacteria enter the liver via the portal circulation and are sterilized, and septic pneumonia occurs in newborns with immature liver immunity. Diabetic frailty is at a high risk of sepsis and is prone to gastrointestinal hypersensitivity such as diabetic diarrhea. In severe periodontal disease, tooth brushing is able to easily cause bacteremia, so it is quite possible that periodontal pathogenic bacterial components invaded in the oral circulation easily reach the kidneys, accumulate in glomeruli with a complex structure of the blood capillary, and cause an inflammatory response through activation of TLRs abnormally expressed in the diabetic environment [3–6].

Recently, it has been strongly suggested that the periodontal pathogenic bacterium *Fusobacterium (F.) nucleatum* may induce inflammation and cancer in the large intestine through the strong activation of TLR2/4 [35–38]. This present study was conducted using diabetic mice and cultured renal tubular epithelial cells to verify the possibility that *F. nucleatum* exacerbates diabetes through induction of SGLT2 overexpression in renal tubules in diabetic mice.

Methods

Animals

This study was designed to investigate the induction of the SGLT2 overexpression with Fn-LPS in murine diabetic renal tubules and diabetes exacerbation. All experiments were conducted in the Fukuoka Dental College Animal Center following the conditions described elsewhere [10, 14–16, 33, 34]. The protocol was approved by the Animal Experiment Committee of Fukuoka Dental

College (No. 19010). The 4-week-old male genetically identical ICR mice were purchased from a commercial vendor (Kyudo, Fukuoka, Japan). The number of mice was decided by rules of the Animal Experiment Committee of Fukuoka Dental College based on the viewpoint of animal welfare [10]. This study used 4 groups (9 mice in each group): non-treated control, Fn-LPS-administered non-diabetic control, diabetic control, and Fn-LPS-administered diabetic experimental. The humane endpoints were daily assessed according to the ARRIVE guidelines and mice reaching humane endpoints were euthanized by induction anesthesia with intraperitoneal injections of sodium pentobarbital and cervical dislocation. In this study, all mice were used as the data included in the experimental and control data, and there were no exclusions. The methods of the production of STZ-induced diabetic mice and of the LPS administration in diabetic mice were described elsewhere [14–16, 33, 34]. Briefly, a single intraperitoneal injection of STZ (200 mg/kg body weight; Sigma-Aldrich Japan, Tokyo, Japan) in a 0.05 M citric acid buffer at pH 4.5 (20 mg/ml) and a single Fn-LPS injection under the buccal mucosa were performed to mice under inhalation anesthesia, and blood glucose concentrations were checked by a Glutest Sensor (Sanwa Kagaku Kenkyusyo CO., LTD., Nagoya, Japan) twice a week after the administrations of STZ and Fn-LPS. Most studies for the STZ-induced murine diabetes model consider blood glucose levels over 300 mg/dL as a sign of diabetes and 50% of mice commonly become diabetic two weeks after STZ administration with blood glucose levels in the 300 to 600 mg/dl range [39, 40]. In this study mice with blood glucose levels above 300 mg/dl were determined to be diabetic, and mice with blood glucose levels above 600 mg/dl were used in the renal immunohistochemical study as the severe diabetic model according to our previous studies [14–16, 33, 34]. The dosage of Fn-LPS (3 mg/kg) was determined according to our previous studies and it was confirmed that the Fn-LPS dosage has no effect on the health condition of these ICR mice (Fig. 1) [33, 34]. There are many reports that the amount of LD50, given all at once, for LPS of the reference strain like *Escherichia* (*E.*) *coli* 0111:B4 (Sigma-Aldrich, St. Louis, MO, USA) which causes the death of one half of a group due to the endotoxin shock caused by intraperitoneal administration to C57BL6 mice at 5–6 weeks of age is approximately 27–30 mg/kg. *Fusobacterium* (*F.*) *nucleatum* is a normal inhabitant of the oral cavity and its proliferation causes periodontitis, but there have been rare cases invade vascular from the oral to cause sepsis worldwide. Since it was assumed that the lethality and physiological toxicity of septic shock by *F. nucleatum* LPS would be much lower than that of *E. coli* LPS, in this experiment the same amount of LPS was administered as in the previous experiment with *P. gingivalis* LPS [41, 42]. Urine and blood samples of diabetic mice with Fn-LPS were collected after euthanasia on the day the mice reached humane endpoints, and of other mice were collected on the day the last diabetic mice with Fn-LPS reached humane endpoints. The samples were analyzed for urine albumin by albumin ELISA kit (Bethyl Laboratories, Inc. Montgomery, Texas, USA), for blood urea nitrogen (BUN) by DetectX (BUN detection kit, Arbor Assays LLC, Ann Arbor, MI, USA), and for blood creatinine (CRE) by LabAssay (Fujifilm Wako Pure Chemical Corporation, Osaka, Japan). Survival curves of control and diabetic mice with/without Fn-LPS were plotted from the day blood glucose levels reached the diabetic range described above.

Cells

This study used the human monocyte-macrophage-like cell line (THP-1, JCRB0112, Japanese Collection of Research Bioresources, Ibaraki, Japan) and mouse monocyte-macrophage-like cell line (J774.1, JCRB0018, Japanese Collection of Research Bioresources) to examine the activity of purified Fn-LPS described below. The cells were cultured in RPMI1640 with 10% fetal calf serum in the usual culture condition. This study also used C57BL/6 mouse primary proximal tubular epithelial cells (C57-6015, Cell Biologics Inc., Chicago, IL) to examine the SGLT2 expression with mouse recombinant TNF-α (R&D Systems Inc., Minneapolis, MN). The cells were cultured in the epithelial cell medium (M6621, Cell Biologics) in the usual culture condition. The MC3T3-E1 cells (RCB1126, RIKEN BioResource Research Center, Tsukuba, Japan) were also used as a negative control for the immunostaining with anti-SGLT2 cultured in α-MEM.

Bacterial culture

F. nucleatum (ATCC 25586) were cultured in Gifu anaerobic medium (Code 05422, Nissui Pharmaceutical Co., Ltd., Tokyo, Japan) in an anaerobic jar for 7 days at 37 °C until the absorbance at OD595 = 1.0, adjusted to 1.0×10^8 CFU /ml and the colonies were counted on the agar plate (Nissui Plate 51041, NK-containing ABHK agar; Shimadzu Diagnostics Corporation, Tokyo, Japan) according to the manufacturer's instructions. Bacterial cells were harvested by the centrifugation at x 4000 x g for 30 min and the pellet was heat-inactivated at 60 °C for 1 h to confirm the absence of growth on the Nissui plate (Shimadzu).

Purification of periodontal pathogen *F. Nucleatum* LPS

This study used *F. nucleatum* (ATCC 25586) to examine the SGLT2 overexpression in the renal proximal tubular epithelial cells with Fg-LPS in vitro and in vivo. The *F. nucleatum* membrane components including LPS

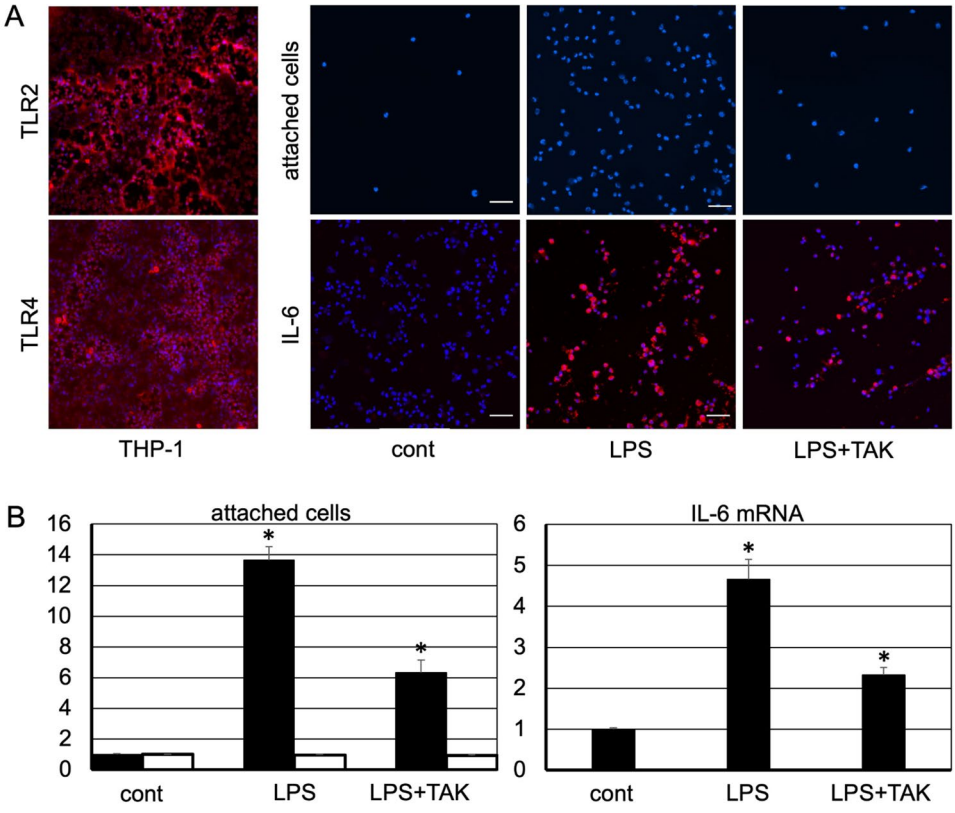

Fig. 1 Analysis for the antigenicity of Fn-LPS to THP-1 cells. **A**. Cell adhesion test and immunostaining by anti-IL-6. Left panels: immunostaining for TLR2 and TLR4 on human monocyte-macrophage-like THP-1 cells cultured without any treatment. It is found that THP-1 cells usually express TLR2 and TLR4. Right top panels: THP-1 cells cultured without any treatment as a control (cont) and with Fn-LPS (LPS) / LPS and TLR4 antagonist TAK-242 (LPS + TAK). Attached cells after the treatment are stained by DAPI in blue. The THP-1 cells are floating cells, attached cell assemblies differentiated into macrophage-like cells are more numerous in the culture of LPS-treated cells than in the control, and there are fewer in culture of LPS + TAK-treated cells than in the culture of LPS-treated cells. Right bottom panels: immunostaining with anti-IL-6 in red on all the cells collected by trypsinization and centrifugation. The nuclei are counterstained by DAPI in blue. The control cells are not stained but the LPS-treated cells are strongly stained. The LPS + TAK-treated cells are immunostained less than the LPS-treated cells. Bar: 100 μm. **B.** Quantitative analysis for the amounts of attached cells and IL-6 mRNA from all cells. The THP-1 cells were cultured without Fn-LPS (LPS) or TLR4 antagonist TAK-242 (TAK) as a control (cont) and cultured with LPS/LPS + TAK. The amounts of attached cells were determined by the absorbance at 450 nm for the medium containing metabolites of a cell counting kit (solid bars). All data were normalized to the amount of control cells and expressed relative to the control in arbitrary units. The amounts of attached cells were larger in LPS-treated cells than in cells without any treatment, and less in LPS + TAK-treated cells than in LPS-treated cells only. The amounts of alive cells in culture with both attached and floating cells were determined by the absorbance of medium containing metabolites of a cell counting kit at 450 nm. There were no significant differences in the number of alive cells among cultures (open bar) and the viability of THP-1 cells was not influenced by LPS and TAK. The antigenicity of LPS to THP-1 cells was also evaluated by the IL-6 mRNA production and the inhibitory effect of TAK. The target gene cDNA from the total cell volumes, attached and floating, in culture were normalized to β-actin cDNA. All data were expressed relative to the control in arbitrary units. The amounts of IL-6 mRNA were for cells with LPS than in cells without any treatment, and smaller in cells with LPS + TAK than in cells with LPS only. *Significantly different from the other two in ANOVA ($P < 0.001$)

termed as Fn-LPS was purified using a LPS extraction kit (iNtRON Biotechnology, Inc., Seongnam, Korea). The activity of purified Fn-LPS was determined by the RT-PCR analysis to determine the increase of interleukin-6 (IL-6) mRNA expression in the THP-1 cells and the inhibition of the IL-6 mRNA production by the TLR4 Inhibitor TAK-242 (Sigma-Aldrich Japan, Tokyo, Japan) which inhibits IL-6 production with IC50 of 1.3 nM. All were performed according to the manufacturer instructions and previous studies [43–45]. The THP-1 cells (1.0×10^8/well) were treated with RPMI1640 culture medium containing LPS (100 ng/ml) or LPS (100 ng/ml) and TAK-242 (1 μM, Sigma-Aldrich Japan) in a 6-well plate for 24 h. After the treatment the attached cells were trypsinized and collected by centrifugation with the floating cells, and the cell pellets were analyzed by real-time PCR described below. The LPS yield was quantified at 545 nm using a ToxinSensor (LAL Endotoxin Assay Kit, GenScript Biotech Corporation, Piscataway, NJ, USA) and a microplate reader.

Cell viability assay

The viabilities of the cells cultured with medium containing LPS (100 ng/ml), TAK-242 (1 μM, Sigma-Aldrich

Japan), and recombinant mouse TNF-α (10 pg/ml, sodium azide free, R&D Systems) were tested using water soluble tetrazolium salts WST-8 (2-(2-methoxy-4-nitrophenyl)-3-(4-nitrophenyl)-5-(2,4-disulfophenyl)-2 H-tetrazolium) of a Cell Counting Kit-8 (Dojindo Molecular Technologies, Inc., Tokyo, Japan). The dosages were determined according to the data sheets and previous studies [46–49]. The nicotinamide adenine dinucleotide produced by intracellular dehydrogenase in mitochondria reduces WST-8 to orange formazan dye via 1-methoxy-5-methylphenazinium methylsulfate. Since the amount of formazan dye as a reduction product of WST-8 is proportional to the number of alive cells, the number was estimated with optical density measurements at the 450 nm wavelength by a microplate reader. Relative viabilities were calculated according to the following formula: absorbance of experimental culture / absorbance of control culture. All data were normalized to controls with no treatment and expressed in arbitrary units.

Cell adhesion assay

The antigenicity of purified Fn-LPS was also determined by the cell adhesion to investigate the number of macrophage-like THP-1 cells differentiated from monocyte-like THP-1 cells cultured with the Fn-LPS and evaluated by the inhibitory effect to the cell adhesion by TAK-242. The THP-1 cells were cultured with LPS (100 ng/ml) or with LPS (100 ng/ml) and TAK-242 (1 μM, Sigma-Aldrich Japan) in a 6-well plate for 24 h. After the treatment the culture medium was removed and washed by new medium five times. The cells attached on the 6-well plate were cultured in the medium containing the substrate of cell counting kit-8 for 4 h and the absorbance of WST-8 metabolizing was measured at 450 nm to determine the number of macrophage-like attached cells differentiated from THP-1. All data were normalized to the control with no treatment and expressed in arbitrary units.

Cell activation assay

The activation of mouse primary proximal tubular epithelial cells by Fn-LPS, TNF-α, and J774.1 cells with Fn-LPS was investigated. The procedures and dosages were determined according to the data sheets and previous studies [15, 33, 34, 46, 47, 50, 51].The tubular cells were cultured in 24-well plates and in 6-well plates on glass cover slips with the medium containing Fn-LPS (100 ng/ml) or TNF-α (10 pg/ml, azide free, ED50: 8–50 pg/m, aa80-235; R&D Systems Inc., Minneapolis, MN), and co-cultured with J774.1 cells supplemented with Fn-LPS (100 ng/ml) in the culture insert (pore size 0.4 μm, Falcon, Thermo Fisher Scientific Inc., Chino, CA). After culturing the SGLT2 production was analyzed by RT-PCR, cell ELISA, and immunostaining as described below.

Table 1 Primer sets

gene	bp	Upper (5`-3`)	Lower (5`-3`)
human IL-6	101	CTGGATTCAATGAGGAGAC TTGCC	CTCACTACTCTCA AATCTGTTCTGGA
mouse IL-6	263	ATGTTCTCTGGGAAATCGTG GAAAT	TCTCTGAAGGACT CTGGCTTTGT
mouse SGLT2	209	CCCATCCCTCAGAAGCAT CTCC	CTCATCCCACAGA ACCAAAGCA
mouse actin-b	441	GTTCTACAAATGTGGCTGA GGA	ATTGGTCTCAAGT CAGTGTACAG
human actin-b	495	ATGTTTGAGACCTTCAACAC	CACGTCACACTTC ATGATGG

Real-time PCR

The real-time PCR was performed to quantify the mRNA expressed amounts of human IL-6 in THP-1 cells and mouse SGLT2 in the cultured mouse renal proximal tubular epithelial cells, and in the mouse kidney tissue using primer sets where the specificities had been confirmed by the manufacturer (Sigma-Aldrich Japan) described elsewhere [15, 16, 33, 34](Table 1). Immediately after excision five mm squares of tissue from mouse kidneys were ground into a paste with a scalpel on glass plates on ice and dissolved in the RLT buffer of an RNeasy kit (Qiagen, Inc., Tokyo, Japan). Also, THP-1 cell pellets collected by centrifugation at 200 x g for 10 min, and the renal proximal tubular epithelial cells attached on the 6-well plate were also dissolved in the RLT buffer of an RNeasy kit (Qiagen). The total RNA extraction from the tissue was performed with a QIAshredder column and an RNeasy kit (Qiagen). When many non-specific bands were identified at the gel electrophoresis after the PCR, a DNAfree kit (Ambion, Huntingdon, UK) was used to remove contaminating genomic DNA. The cDNA samples were analyzed by RT-PCR to quantify the mRNA amounts with 50 pM of primer sets. The cDNA (1 μl) was amplified in a 25 μl volume of Power-SYBR Green PCR Master Mix (Applied Biosystems, Foster City, CA, USA) in a Stratagene Mx3000P real-time PCR system (Agilent Technologies, Inc., Santa Clara, CA, USA) and the fluorescence was monitored at each cycle. Cycle parameters were 95˚C for 15 min to activate Taq followed by 40 cycles of 95˚C for 15s, 58˚C for 1 min, and 72˚C for 1 min. Two standard curves were created for the real-time analysis from amplicons for β-actin and target genes in three serial 4-fold dilutions of cDNA. The β-actin/SGLT2/IL-6 gene cDNA levels in each of the samples were quantified with β-actin/SGLT2/IL-6 standard curves by allowing the Mx3000P software to accurately determine each cDNA unit. Finally, the target gene cDNA amounts in each sample were normalized to β-actin cDNA. All data were normalized to controls with no treatment and expressed in arbitrary units.

Cell ELISA

The ELISA to examine the induction of SGLT2 in proximal tubular epithelial cells (C57-6015, Cell Biologics) by Fn-LPS, TNF-α, and J774.1 cells with Fn-LPS was performed according to the method described elsewhere [33]. The cells with the treatment in 24-well plates described above were fixed in 100% methanol for 5 min at -20˚C followed by treatment with 0.5 µl of PBS blocking solution containing goat serum (0.1%) for 30 min at 20˚C and then with 0.5 µl of blocking solution containing rabbit anti-mouse SGLT2 (1 µg/ml of #ab85626, Abcam plc., Cambridge, UK) for 8 h at 4˚C. After the primary antibody treatment, the sections were washed three times in PBS for 10 min, treated with 0.5 ml of blocking solution containing a peroxidase-conjugated second antibody (0.1 µg/ml, Vector Elite ABC kit; Vector Laboratories, Burlingame, CA) for 1 h at 20˚C, reacted with a TMB kit (volume 0.18 ml; Thermo Fisher Scientific, Inc., Waltham, MA) at room temperature, and then the absorbance changes at 450 nm were measured by a microplate reader. The relative production amounts of SGLT2 protein were evaluated by the absorbance of TMB metabolizing and normalization to the control, expressed in arbitrary units.

Immunohistochemistry

The procedure was performed according to the method described elsewhere [15, 33, 34]. The frozen 10 µm mouse kidney tissue sections cut in a cryostat on slide glass were fixed in 100% methanol for 5 min at -20˚C. The sections were rinsed by 10 mM PBS and immersed in the PBS blocking solution containing goat serum (0.1%) for 30 min at 20˚C, and then double immunostained with a rabbit polyclonal anti-mouse SGLT2 (#ab85626, Abcam plc., Cambridge, UK) to discriminate proximal tubules and a hamster monoclonal anti-mouse podoplanin clone 8.8.1 (#127402, BioLegend Inc., San Diego, CA, USA) to distinguish renal glomerular podocytes and macrophages [34]. The sections were treated with blocking solution containing primary antibodies (1 µg/ml) for 8 h at 4˚C. After the treatment the sections were washed three times in PBS for 10 min and immunostained for 1 h at 20˚C with Alexa Fluor 488/568-conjugated goat anti- hamster/rabbit IgGs (0.1 µg/ml, Probes Invitrogen Com., Eugene, OR). The sections were mounted in 50% polyvinylpyrrolidone solution and examined by microscope digital camera systems with CFI Plan Apo Lambda lens series and DS-Ri2/Qi2 (Nikon Corp., Tokyo, Japan). All experiments were repeated three times with several sections.

For the cultured cells, THP-1 and tubular cells were immunostained by anti-IL-6 and by anti-SGLT2. The monocyte-like THP-1 cells floating in the medium were harvested by centrifugation. Since the macrophage-like THP-1 cells activated by Fn-LPS were attached in the 6-well plate, the cells were trypsinized and harvested by the centrifugation. The cell pellets were resuspended in PBS and the cell suspension (10 µl) was placed on slide glass and air dried. The mouse renal proximal convoluted tubular cells cultured on glass cover slips were also air dried. The cells on the glass were fixed in 100% methanol for 5 min at -20˚C, rinsed by 10 mM PBS, and then immersed in the PBS blocking solution containing goat serum (0.1%) for 30 min at 20˚C. After blocking, cells were exposed to primary antibodies (1 µg/ml) diluted in the blocking agent for 8 h at 4˚C. The THP-1 cells were treated with a rabbit polyclonal anti-human IL-6 (1 µg/ml, #ab6672; Abcam plc., Cambridge, UK) and mouse proximal tubular cells were treated with rabbit polyclonal anti-mouse SGLT2 (#ab85626, Abcam plc., Cambridge, UK). After the treatment cells were exposed to secondary antibodies (0.1 µg/ml): Alexa Fluor 488/568-conjugated goat anti-rabbit IgG (Probes Invitrogen). Cell nuclei were counterstained with 4', 6-diamidino-2-phenylindole (DAPI). The immunostained sections were examined by microscope digital camera systems with a CFI Plan Apo Lambda lens series and DS-Ri2/Qi2 (Nikon Corp., Tokyo, Japan).

Measurements of the immunostained areas of tissue sections

The SGLT-positive glomeruli immunostained by anti-SGLT2 (Abcam) were counted by fluorescence microscopy (BZ-810; Keyence Corp., Osaka, Japan). The proximal convoluted tubules where the luminal side was reacted with anti-SGLT2 (Abcam) were also counted and determined as tubules in the SGLT2 overexpression. Relative numbers of the SGLT-2-positive organs were expressed as arbitrary units according to the formula of the normalization to the ICR control: the number of organs in Fn-ICR, STZ-ICR or Fn-STZ / ICR. All experiments were repeated at least five times.

Statistics

Animal experiments were done with 36 mice of 4 groups (9 mice in each group) as described above. All experiments for immunohistochemistry, RT-PCR and ELISA were repeated five times. Data were expressed as the mean + SD and mean values were calculated with standard deviations. The statistical significance of differences ($P < 0.01$) was determined by one-way ANOVA and two-tailed unpaired Student's t test with STATVIEW 4.51 software (Abacus concepts, Calabasas, CA, USA). The corresponding author is fully aware of the group allocation at the different stages of the experiments. The data analysis and assessments were performed by all co-authors.

Results

Antigenicity of purified Fn-LPS

It was confirmed that THP-1 cells usually express TLR2 and TLR4. The number of macrophage-like cells attached on the culture plate was significantly increased with Fn-LPS in monocyte-like floating THP-1 cells and the increase was suppressed by the TLR4 inhibitor (Fig. 1). The produced amount of IL-6 mRNA in THP-1 cells was also significantly increased with Fn-LPS and the production was suppressed by the TLR4 inhibitor. The viability of THP-1 was not influenced by Fn-LPS or TLR4 inhibitor.

Expression of SGLT2 in the cultured tubular epithelial cells

The tubular epithelial cells without any treatment and the cells cultured with Fn-LPS or co-cultured with J774.1 were rarely immunostained by anti-SGLT2, whereas the tubular epithelial cells cultured with TNF-α were immunostained by anti-SGLT2 as well as the cells co-cultured with Fn-LPS-supplemented J774.1 cells (Fig. 2). The viability of proximal tubular epithelial cells was not influenced by the experiment. There was no difference in the SGLT2 protein production amounts between tubular epithelial cells without any treatment and the cells cultured with Fn-LPS or co-cultured with J774.1, whereas the protein amounts were significantly larger in the cells with TNF-α than in the cells with Fn-LPS or co-cultured with J774.1 (Fig. 2). Moreover, the SGLT2 protein production amounts were significantly larger in the cells co-cultured with Fn-LPS-supplemented J774.1 cells than in the cells with TNF-α only (Fig. 2). There was no difference in the mRNA amounts of SGLT2 between tubular epithelial cells and the cells with Fn-LPS or co-cultured with J774.1, whereas the mRNA amounts in the tubular epithelial cells were significantly larger in the cells with TNF-α than in the cells with Fn-LPS or co-cultured with J774.1 (Fig. 2). Moreover, the mRNA amounts of SGLT2 were also significantly larger in the cells co-cultured with

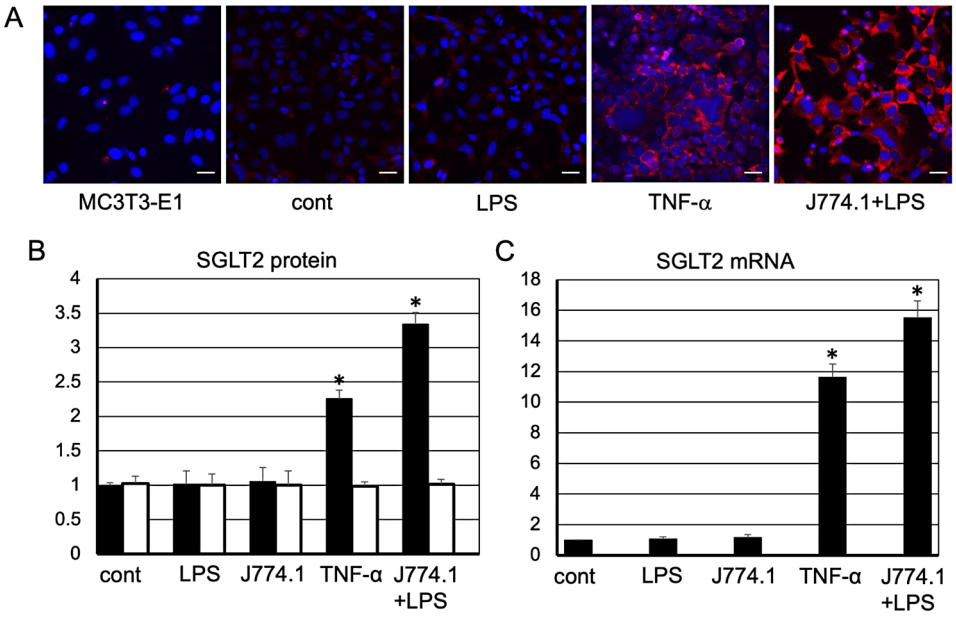

Fig. 2 Expression of SGLT2 in cultured mouse primary proximal tubular epithelial cells. **A**. Immunostaining by anti-SGLT2. Cells cultured on glass slips were immunostained by anti-SGLT2 in red and nuclei were counterstained by DAPI in blue. The negative control MC3T3-E1 cells were not immunostained by SGLT-2. The untreated tubular epithelial cells (cont) and the cells cultured with Fn-LPS (LPS) were rarely immunostained by anti-SGLT2. The tubular epithelial cells cultured with TNF-α were strongly immunostained by anti-SGLT2 as well as the cells co-cultured with Fn-LPS-supplemented J774.1 cells (J774.1 + LPS). Bar: 100 μm. **B.** Cell ELISA analysis for the expression of SGLT2 protein. The produced amounts of SGLT2 protein (closed bars) were determined by the mean absorbance of TMB metabolizing at 450 nm. All data were expressed relative to the control cells cultured without any treatment (cont) in arbitrary units. The amounts of alive cells in culture with both attached and floating cells were also determined by the absorbance of medium containing metabolites of a cell counting kit at 450 nm. There was no significant difference in the number of alive cells among culture (open bars) and the viability of proximal tubular epithelial cells was not influenced by the experiment. There was no difference in the SGLT2 protein amounts between the control tubular epithelial cells, the control cells with Fn-LPS (LPS) or the control cells co-cultured with J774.1. The SGLT2 protein amounts were significantly larger in the cells with TNF-α than in the controls. The SGLT2 protein amounts were also significantly larger in the cells co-cultured with Fn-LPS-supplemented J774.1 cells (J774.1 + LPS) than in the cells with TNF-α. *Significantly different compared to the other four in ANOVA ($P < 0.001$). **C**. real time-PCR analysis for the SGLT2 mRNA. The target gene cDNA amounts were normalized to β-actin cDNA. All data were expressed relative to the control cells cultured without any treatment (cont) in arbitrary units. There was no difference in the mRNA amounts of SGLT2 between tubular epithelial cells and the cells with Fn-LPS (LPS) or co-cultured with J774.1. The mRNA amounts of SGLT2 in the tubular epithelial cells were significantly larger in the cells with TNF-α than in the cells with LPS. The mRNA amounts of SGLT2 in the tubular epithelial cells was also significantly larger in the cells co-cultured with Fn-LPS-supplemented J774.1 cells (J774.1 + LPS) than in the cells with TNF-α. *Significantly different compared to the other four in ANOVA ($P < 0.001$)

Fn-LPS-supplemented J774.1 cells than in the cells with TNF-α only (Fig. 2).

Changes of blood glucose, BUN, CRE levels and survival curves

The time to reach diabetic condition where the blood glucose level reaches over 300 mg/dl was shorter in mice administered with both STZ and Fn-LPS than in mice administered with STZ only, and the rise for the blood glucose level was significantly steeper in mice administered with both STZ and Fn-LPS than in mice administered with STZ only (Fig. 3). The mean of blood glucose levels was statistically significantly higher than in mice administered with both STZ and Fn-LPS than in mice with STZ only (Fig. 3). Urine albumin, and blood BUN and CRE were significantly higher in the diabetic mice administered Fn-LPS than in the diabetic mice not administered Fn-LPS and other mice (Fig. 4). For the survival curve all of the mice with both STZ and Fn-LPS reached humane endpoints during the survival period of all of the mice administered Fn-LPS/STZ only (Fig. 4).

Expression of SGLT2 in the mouse renal tissue

The reaction products of immunostaining with anti-SGLT2 were rare in the renal tissue of control mice both with no treatment and with Fn-LPS alone whereas the strong immunostaining with anti-SGLT2 was observed in the renal tissue of diabetic mice and those with Fn-LPS administration (Fig. 5). Reaction products with anti-SGLT2 were observed in the glomeruli and renal proximal tubules of the diabetic mice and those administered Fn-LPS (Fig. 6). In the diabetic mice the reaction products with anti-SGLT2 were observed in the cytoplasm near the outer wall of the proximal tubules whereas in the diabetic mice with Fn-LPS the reaction products with anti-SGLT2 were observed in the cytoplasm both near the outer wall and at the inner wall of the proximal tubules with diffused reaction products in the lumen (Fig. 7). The promotion of the SGLT2 expression at the inner lumen of proximal tubules were stronger in the Fn-LPS-administered-diabetic mice than in diabetic mice. Inflammatory podoplanin-positive macrophages were observed, and the tissue appears to be nephropathic because secretions filled the lumen of the damaged tubules (Fig. 7). The reaction products with anti-podoplanin were also observed on macrophages. In the quantitative analysis for the SGLT2 mRNA expression in the mouse renal tissue the expression was higher in the diabetic mice than in healthy mice and in mice administered Fn-LPS, whereas the amount was higher in the diabetic mice administered Fn-LPS than in the diabetic mice (Fig. 8). The number of glomeruli with reaction products to anti-SGLT2 was more common in the diabetic mice than in healthy mice and in Fn-LPS-administered mice, while there was no statistically significantly difference between the diabetic mice and the Fn-LPS-administered

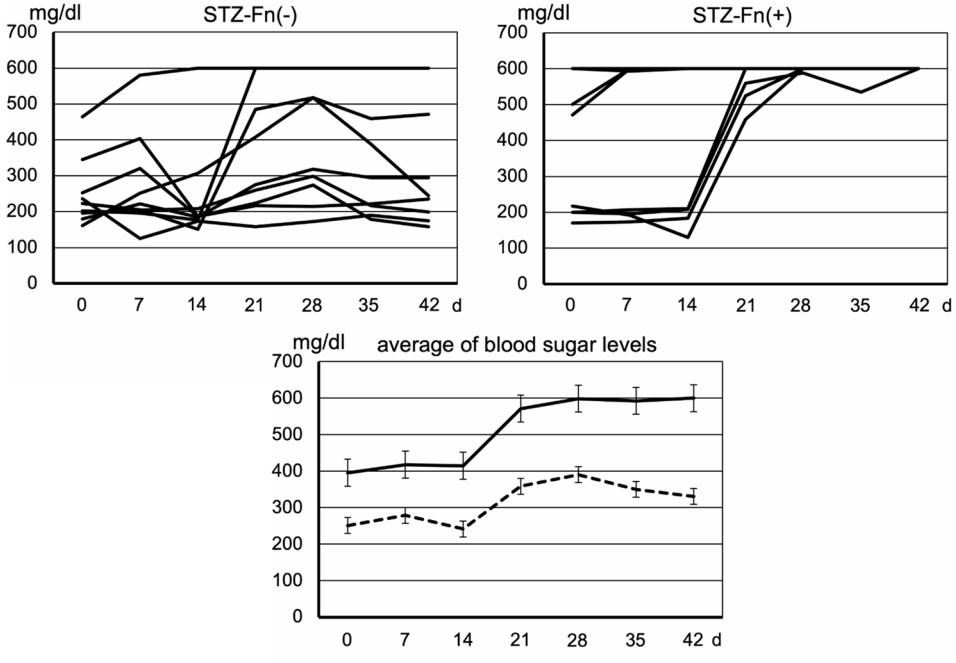

Fig. 3 Quantitative analysis of blood sugar levels. The increase of blood glucose was steeper in mice administered with STZ and Fn-LPS (solid lines) than in mice administered with STZ only (dashed line). The mean time to reach diabetic condition (300 mg/dl of blood glucose) was shorter in mice administered with both STZ and Fn-LPS than in mice administered with STZ only. The mean of blood glucose levels was statistically significantly higher than in mice administered with both STZ and Fn-LPS than in mice administered with STZ only

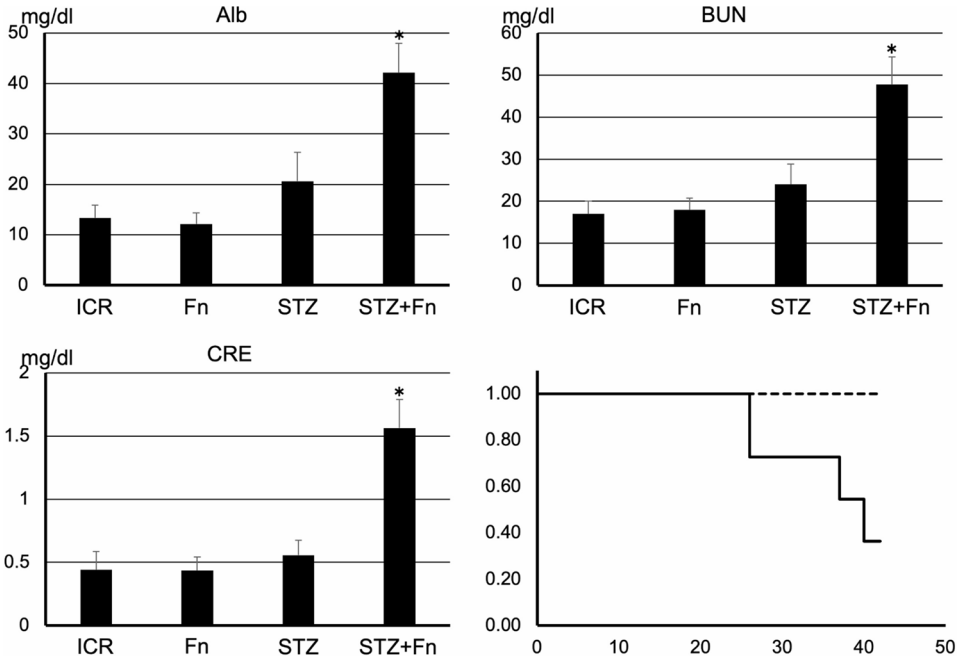

Fig. 4 Quantitative analysis of blood BUN and CRE, and survival curves. Urine and blood samples of diabetic mice with Fn-LPS were collected after euthanasia on the day the mice reached humane endpoints, and of other mice were collected on the day the last diabetic mice with Fn-LPS reached humane endpoints. The samples were analyzed for urine albumin, blood urea nitrogen (BUN), and for blood creatinine (CRE). Albumin, BUN and CRE were significantly higher in the diabetic mice administered Fn-LPS than in the diabetic mice not administered Fn-LPS and other mice. Survival curves of control and diabetic mice with/without Fn-LPS were plotted from the day blood glucose levels reached the diabetic range described above. The survival curve showed that all of the mice with both STZ and Fn-LPS (solid line) reached humane endpoint during the survival period of all of the mice administered STZ/Fn-LPS only (dashed line). Values are mean ± SE. *Significantly different compared to the other four in ANOVA ($P < 0.001$)

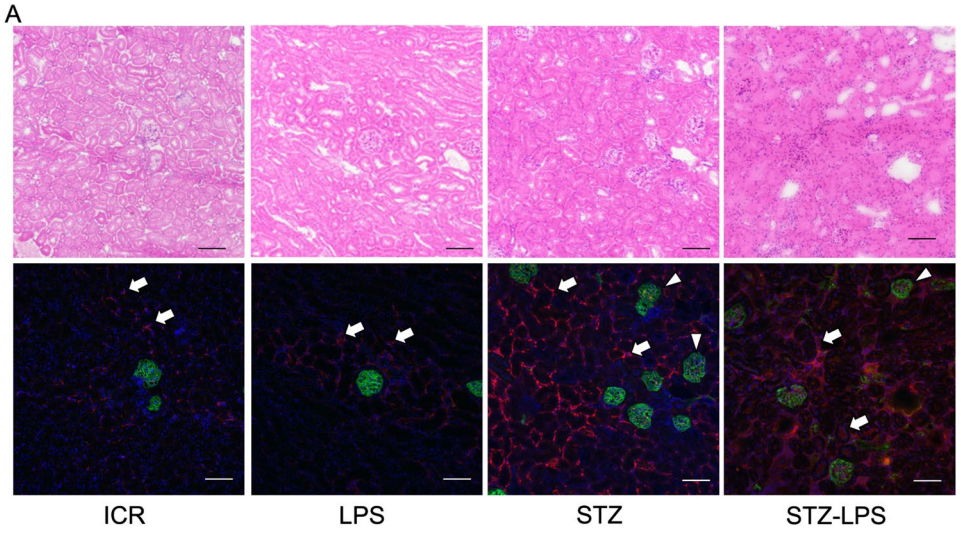

Fig. 5 The renal SGLT2 expression in the mouse tissue The renal tissue sections were immunostained by anti-podoplanin to demonstrate glomeruli in green and by anti-SGLT2 in red. Top panels are HE stained. Sections were counterstained to nuclei by DAPI in blue. The reaction with anti-SGLT2 was very weak in control mice without any treatment (ICR) and in mice with Fn-LPS only (LPS), whereas there was a strong reaction with anti-SGLT2 in the STZ-induced diabetic mice (STZ) and in the diabetic mice with LPS (STZ-LPS). Bar: 100 μm

diabetic mice. The number of renal proximal tubules with reaction products to anti-SGLT2 at the luminal side was more common in the Fn-LPS-administered diabetic mice than in healthy mice, in diabetic mice, and in mice administered Fn-LPS only.

Discussion

Induction of SGLT2 by *F. Nucleatum* LPS in the cultured tubular epithelial cells

P. gingivalis is the most important periodontal pathogens that have been studied for the association between

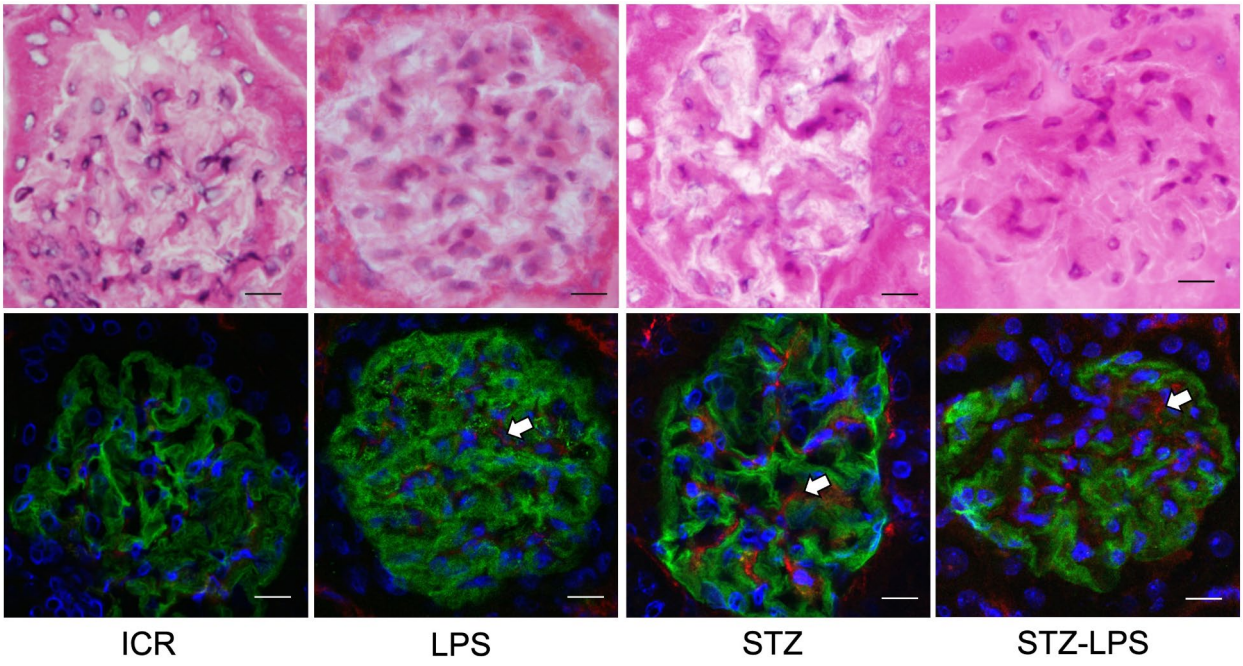

Fig. 6 SGLT2 distribution in glomeruli The renal tissue sections were immunostained by anti-podoplanin to demonstrate glomeruli in green and by anti-SGLT2 in red. Top panels are by HE staining. Sections were counterstained to nuclei by DAPI in blue. No reaction to anti-SGLT2 was observed in glomeruli of the control mice (ICR) and in mice administered Fn-LPS only (LPS), while there was reaction in glomeruli in the STZ-induced diabetic mice (STZ) and in the LPS-administered diabetic mice (STZ-LPS). Bar: 100 μm

periodontal disease and circulatory and renal disorders in immunocompromised patients [33, 34]. However, *P. gingivalis* LPS activates TLR2 but TLR4 very weakly, and it has been reported that *P. gingivalis* LPS binding to TLR masks non-specific defense mechanisms. In recent years, many researchers reported the induction of cancer and inflammation in the large intestine due to the activation of TLR4 by *F. nucleatum* [35–38]. Therefore, our findings that *F. nucleatum* may aggravate diabetes and induce nephropathy are significant in elucidating the relationship between the progression and complications of diabetes and periodontitis. Experimental antigenicity and clinical pathogenicity of heat-inactivated *F. nucleatum* including LPS has been reported [38, 43, 44]. It is also well known that there is induction of IL-6 and TNF-α by sensing LPS via TLR4 in the mouse and human monocyte-macrophage like cell line J774.1 and THP-1 [43, 44, 51]. In the test for the antigenicity of purified Fn-LPS, the adhesive macrophage-like cells differentiated from the floating monocyte like THP-1 cells with expressing TLR2 and TLR4 were significantly increased with Fn-LPS and the differentiation was suppressed by the TLR4 inhibitor, indicating that the purified Fn-LPS enables stimulating of monocytes via TLR4 (Fig. 1). The produced amount of IL-6 mRNA in THP-1 cells was significantly increased with Fn-LPS and the induction was counteracted by the TLR4 inhibitor, indicating that the antigenicity of the purified Fn-LPS in this study is useful as a TLR4 ligand (Fig. 1). It has been reported that the production of SGLT2 in tubular epithelial cells increases by inflammatory cytokines like IL-6 and TNF-α [50]. In the cultured proximal tubular epithelial cells, the expression of SGLT2 was not influenced by Fn-LPS but induced by culturing with TNF-α, further, the cells co-cultured with Fn-LPS-supplemented monocyte like mouse J774.1 cells expressed SGLT2 more strongly than the cells cultured with TNF-α (Fig. 2). In our previous studies the expression of TLR2/4 are usually not observed in glomeruli and tubular epithelial cells while it has been reported in human and murine somatic tissue with the diabetic condition [14, 15]. There have been also reports that inflamed tubular epithelial cells produce inflammatory cytokines by sensing pathogens via TLR4 [20, 52, 53]. These suggest that the SGLT2 expression is induced by several inflammatory cytokines including at least TNF-α derived from immunocytes like macrophages sensing Fn-LPS via TLR4. The overexpression of SGLT2 may also occur through recognition of Fn-LPS by TLR4 expressed on tubular epithelial cells themselves in the somatic tissue under diabetic conditions.

Effect of Fn-LPS to blood glucose control

There are reports suggesting that periodontal disease is an important risk factor for diabetic exacerbation from the standpoint of the periodontal-systemic circulation [3–7]. We previously demonstrated a model of diabetes

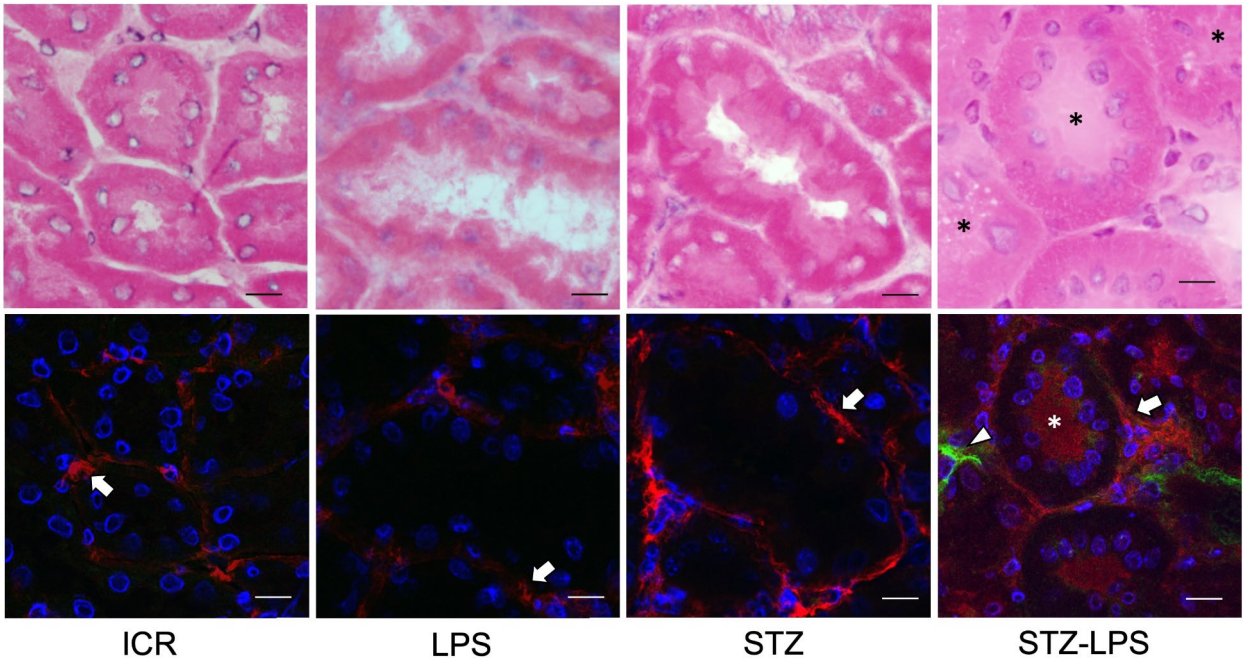

Fig. 7 SGLT2 distribution proximal tubules The renal tissue sections were immunostained by anti-podoplanin to demonstrate macrophages in green and by anti-SGLT2 in red. Top panels are by HE staining. Sections were counterstained to nuclei by DAPI in blue. The immunoreaction to anti-SGLT2 was very weak in renal proximal tubules in the control mice (ICR) and in mice administered Fn-LPS only (LPS), while there was a strong reaction with anti-SGLT2 (arrows) in STZ-induced diabetic mice (STZ) and in the LPS-administered diabetic mice (STZ-LPS). The immunoreaction with anti-SGLT2 in the proximal tubules of the diabetic mice was mainly observed in the cytoplasm near the basal side (arrows). In the LPS-administered diabetic mice reaction with anti-SGLT2 in the proximal tubules was observed in the cytoplasm at the inner side and there was significant diffusion of reaction products with anti-SGLT2 in the lumen of the proximal tubules (asterisk). The tissue appears to be nephropathic based on findings that reaction products with anti-podoplanin were also observed on macrophages in green (arrowhead), and that reaction products with anti-SGLT2 fill the lumen of the damaged proximal tubules (asterisks in HE). Bar: 100 μm

exacerbation induced by *P. gingivalis* LPS, but the ability of *P. gingivalis* LPS to activate TLR4 was very weak, therefore, we have been sought to identify periodontal pathogens that contribute more strongly to the exacerbation of diabetes than *P. gingivalis* [16, 33]. In this present study, the Fn-LPS administration under the buccal mucosa of the diabetic model mice shortened the time to reach diabetic conditions with the steep rise of blood glucose levels comparing with usual diabetic model mice (Fig. 3). This may suggest that the infection of *F. nucleatum* in periodontal disease enables acceleration of the exacerbation of diabetes. We have reported that *P. gingivalis* LPS caused the severe diabetic nephropathy due to the abnormal immunoreaction of TLR2 in the renal tissue of diabetic model mice [16]. It has been reported that the detected level of *F. nucleatum* is higher in patients with uncontrolled diabetes than in patients without diabetes, and that *F. nucleatum* causes TLR4-mediated strong inflammation, such as fetal demise [54] and large intestine [35–38]. Since urine albumin, and blood BUN and CRE were significantly higher in the diabetic mice administered Fn-LPS than in the diabetic mice not administered Fn-LPS and other mice, it is thought that *F. nucleatum*-associated renal inflammation is not only an exacerbation factor of diabetes but also a risk factor provoking diabetic nephropathy (Fig. 4). All of the Fn-LPS-administered diabetic mice reached humane endpoints during the survival period of all of the diabetic mice and the Fn-LPS-administered mice, indicating that Fn-LPS became a lethal factor in STZ-administered mice in the diabetic condition (Fig. 4).

Effect of Fn-LPS to the SGLT2 expression in the renal tissue

We have reported that *P. gingivalis* LPS occurs the abnormal accumulations of the several molecules including SGLT2 in diabetic mouse kidneys and induces severe nephropathy [14–16, 33, 34]. In the immunohistochemical study,

the SGLT2 expression was rarely observed in healthy mice with/without Fn-LPS but the expression was found in diabetic mice and in Fn-LPS-administered diabetic mice both in renal proximal tubules (Fig. 5) and also in glomeruli (Fig. 6). Considering the results of in vitro experimental models (Fig. 2), these may suggest that the abnormal SGLT2 expression was induced by the inflammatory cells or inflamed glomerular and tubular cells themselves sensing Fn-LPS via TLR2/4 under diabetic conditions. It has been reported that the SGLT2

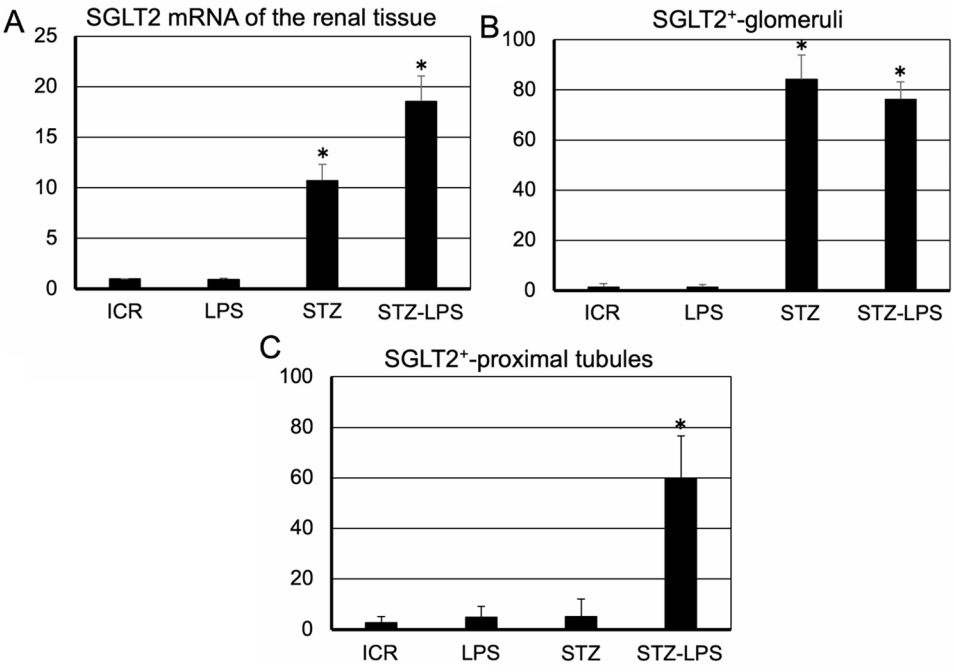

Fig. 8 Quantitative analysis for the SGLT2 expression in the mouse tissue **(A)** Real time-PCR. The SGLT2 mRNA amounts of the renal tissue was higher in the STZ-induced diabetic mice (STZ) than in healthy control mice without any treatment (ICR) and in the Fn-LPS-administered mice (LPS). The SGLT2 mRNA amounts were also higher in the Fn-LPS-administered diabetic mice (STZ-LPS) than in the diabetic mice. The target gene cDNA amounts were normalized to β-actin cDNA and all data were expressed relative to controls in arbitrary units. *Significantly different compared to the other three in ANOVA ($P < 0.001$). **(B)** Number of SGLT2-expressed glomeruli. The number of glomeruli with reaction products to anti-SGLT2 was larger in the STZ-induced diabetic mice (STZ) than in the healthy control mice without any treatment (ICR) and in the Fn-LPS-administered mice (LPS), while there is no statistically significantly difference between the diabetic mice and the Fn-LPS-administered diabetic mice (STZ-LPS). All data are expressed relative to controls in arbitrary units. *Significantly different compared to the other two groups by ANOVA ($P < 0.001$). **(C)** Number of SGLT2-expressed proximal tubules. The number of renal proximal tubules with reaction products to anti-SGLT2 both in the cytoplasm at the inner side and in the lumen was more in the Fn-LPS-administered diabetic mice (STZ-LPS) than in healthy control mice without any treatment (ICR), in the Fn-LPS-administered mice (LPS), in the STZ-induced diabetic mice (STZ). All data are expressed relative to controls in arbitrary units. *Significantly different compared to the other three in ANOVA ($P < 0.001$)

expression occurs at the brush border in renal proximal tubule epithelial cells [55, 56]. However, it seems natural that in a healthy state SGLT2 is rarely expressed at a detection level of immunostaining because the overexpression reads to be hyperglycemia. Further, the SGLT2 accumulation on the basal side of proximal tubules significantly increased in the diabetic mice and transport to the luminal side and the significant diffusion of SGLT2 in the lumen occurred in the mice with severe diabetic exacerbation and nephropathy by Fn-LPS (Fig. 7). It was thought that SGLT2 in the rough endoplasmic reticulum near the nucleus is first stored on the basal side and then moves to the luminal side to play a role in the reabsorption of glucose flowing through the renal tubule [55, 56]. Furthermore, in the nephropathic kidneys of severely diabetic mice, many podoplanin-positive macrophages were observed between tubules (Fig. 7). The Fn-LPS may contribute to the abnormal overexpression of SGLT2 due to the inflammatory response of inflamed tubular cells or immunocytes sensing Fn-LPS. The renal SGLT2 mRNA amounts were higher in the diabetic mice than in healthy mice with/without Fn-LPS, and the mRNA amounts in the diabetic mice increased significantly by the Fn-LPS (Fig. 8). Further, the number of proximal tubules with SGLT2 expression at the inner wall and the significant diffusion of SGLT2 in the lumen of the diabetic mice increased significantly by the Fn-LPS although there was no difference in the glomerular SGLT expression by Fn-LPS administration (Fig. 8). From these above results, it is thought that *F. nucleatum* LPS may accelerate the promotion of SGLT expression by the inflammatory response of the tubular cells themselves and intertubular macrophages which increased susceptibility to infection under diabetic circumstances.

Oral bacterial components enter the systemic circulation and spread to the whole body, and the immunoreaction complexes with the components accumulate in the kidneys while intestinal inhabitants enter the liver via the enterohepatic circulation and are immediately sterilized [3–7].

The glomerular capillaries rarely express TLR2/4 in the healthy condition but strongly express them under diabetic conditions, and produce inflammatory cytokines by sensing the periodontal pathogen derived from the circulation via abnormally expressed TLR2/4, and

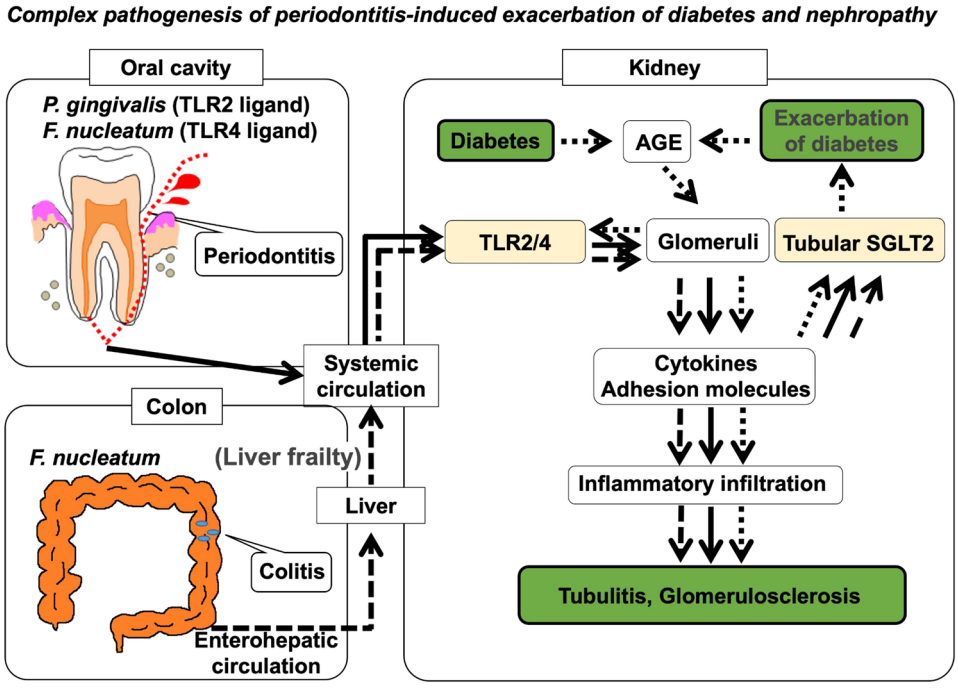

Fig. 9 Complex pathogenesis of periodontitis-induced exacerbation of diabetes and nephropathy The AGEs generated in the diabetic condition and flowing through the circulatory system accumulate in glomeruli and induce unusual TLR2/4 expressions (dotted line). If diabetic patients have periodontal disease (solid line) or colonic and liver frailty (dashed line), periodontitis-derived pathogens that enter the glomeruli from the circulatory system induce the production of inflammatory cytokines and leukocyte adhesion molecules in renal organs and immunocytes recognizing pathogens via TLR2/4

finally causes diabetic nephropathy [10–13, 33, 34, 48, 57] (Fig. 9).

Since it has been reported that *F. nucleatum* shows TLR4-associated strong pathogen, it may be postulated that the cell membrane components derived from *F. nucleatum* LPS cause renal inflammatory reactions through the recognition by overexpressed TLR4 on the glomeruli and leukocytes under renal diabetic conditions and induces the production of inflammatory cytokines which accelerate the abnormal expression of SGLT2 in glomeruli and renal proximal tubules [35–38](Fig. 9).

The SGLT2 accumulates without being metabolized due to renal dysfunction, and inflammatory cytokines like IL-6 and TNF-α progressively induce SGLT2 overexpression in diabetic kidneys as nephritis progresses [8, 9, 38, 58, 59]. Altogether this present study may suggest that the proximal tubular epithelial cells could abnormally upregulate the SGLT2 expression by sensing *F. nucleatum* LPS in patients with increased susceptibility to infection under the diabetic condition and cause the tubulointerstitial nephritis (Fig. 9). Since SGLT2 increases in diabetic patients with persistent hyperglycemia, periodontitis-induced SGLT2 overexpression may be a serious diabetes exacerbating factor.

Conclusions

The results suggest that renal diabetic inflammatory events in the presence of pathogens derived from *F. nucleatum* accelerate the expression of SGLT2 in the proximal tubules. Periodontal care may prevent the exacerbation of diabetes by the suppression of inflamed overexpression of renal SGLT2.

Abbreviations

TLR	toll-like receptor
LPS	lipopolysaccharide
F. nucleatum	Fusobacterium nucleatum
STZ	streptozotocin
Fn-LPS	Fusobacterium nucleatum lipopolysaccharide
SGLT2	sodium-glucose cotransporter 2
HE	haematoxylin and eosin
DAP1	4′, 6-diamidino-2-phenylindole

Acknowledgements

Not applicable.

Author contributions

YS conceived this study; YS designed the study and wrote the manuscript; AS and YS undertook the statistical analyses; AS, KK and YS acquired the data, edited, and approved the manuscript. AS and YS prepared figures. All authors reviewed the manuscript and consented to the publication.

Funding

This work was supported in part by Grant-in-Aid for Scientific Research (B) 23K24560 (principal investigator: Sawa, Y), Grant-in-Aid for Challenging Research (Exploratory) 22K19623 (principal investigator: Sawa, Y.) and Grant-in-Aid for Scientific Research (C) 23K09474 (principal investigator: Kajiwara, K) from the Japan Society for the Promotion of Science. None of the organizations providing the funding participated in or influenced the design

of the study, the collection, analysis, and interpretation of data, or the writing of the manuscript.

Data availability

The datasets generated and/or analyzed during the current study are not publicly available due to the need to keep them confidential but are available from the corresponding author on request.

Declarations

Ethical approval

All methods were performed in accordance with the relevant guidelines and regulations. The animal experimental procedures were prepared following the ARRIVE guidelines. The protocol of the experiments for animal use was approved by the Animal Experiment Committee of Fukuoka Dental College (No. 19010). For studies with human subjects, include the statement "All procedures followed were in accordance with the ethical standards of the responsible committee on human experimentation (institutional and national) and/or with the Helsinki Declaration of 1964 and later versions.

Consent to participate

Not applicable.

Consent to publish

Not applicable.

Competing interests

The authors declare no competing interests.

Author details

[1]Dentistry and Pharmaceutical Sciences, Okayama University Graduate School of Medicine, 2-5-1 Shikata-cho, Kita-ku, Okayama 700-0914, Japan
[2]Department of Oral Growth & Development, Fukuoka Dental College, 2- 15-1 Tamura, Sawara-ku, Fukuoka 814-0193, Japan
[3]Department of Oral Function & Anatomy, Dentistry and Pharmaceutical Sciences, Okayama University Graduate School of Medicine, 2-5-1 Shikata-cho, Kita- ku, Okayama 700-0914, Japan
[4]Department of Dental Anesthesiology & Special Care Dentistry, Dentistry and Pharmaceutical Sciences, Okayama University Graduate School of Medicine, 2-5- 1 Shikata-cho, Kita-ku, Okayama 700-0914, Japan

Received: 4 August 2024 / Accepted: 14 January 2025
Published online: 24 January 2025

References

1. Antonetti DA, Klein R, Gardner TW. Diabetic retinopathy. N Engl J Med. 2012;366(13):1227–39. https://doi.org/10.1056/nejmra1005073.
2. Alicic RZ, Rooney MT, Tuttle KR. Diabetic kidney disease: challenges, progress, and possibilities. Clin J Am Soc Nephrol. 2017;12(12):2032–45. https://doi.org/10.2215/cjn.11491116.
3. Liccardo D, Cannavo A, Spagnuolo G, Ferrara N, Cittadini A, Rengo C, Rengo G. Periodontal Disease: a risk factor for diabetes and cardiovascular disease. Int J Mol Sci. 2019;20(6). https://doi.org/10.3390/ijms20061414.
4. Garcia RI, Henshaw MM, Krall EA. Relationship between periodontal disease and systemic health. Periodontol 2000 2001; 25:21–36. https://doi.org/10.1034/j.1600-0757.2001.22250103.x
5. Olsen I. From the Acta Prize lecture 2014: the periodontal-systemic connection seen from a microbiological standpoint. Acta Odontol Scand. 2015;73(8):563–8. https://doi.org/10.3109/00016357.2015.1007480.
6. Otomo-Corgel J, Pucher JJ, Rethman MP, Reynolds MA. State of the science: chronic periodontitis and systemic health. J Evid Based Dent Pract. 2012;12(3 Suppl):20–8. https://doi.org/10.1016/s1532-3382(12)70006-4.
7. Wu T, Trevisan M, Genco RJ, Dorn JP, Falkner KL, Sempos CT. Periodontal disease and risk of cerebrovascular disease: the first national health and nutrition examination survey and its follow-up study. Arch Intern Med. 2000;160(18):2749–55. https://doi.org/10.1001/archinte.160.18.2749.
8. Yaribeygi H, Butler AE, Atkin SL, Katsiki N, Sahebkar A. Sodium-glucose cotransporter 2 inhibitors and inflammation in chronic kidney disease: possible molecular pathways. J Cell Physiol. 2018;234(1):223–30. https://doi.org/10.1002/jcp.26851.
9. Wang XX, Levi J, Luo Y, Myakala K, Herman-Edelstein M, Qiu L, Wang D, Peng Y, Grenz A, Lucia S, et al. SGLT2 protein expression is increased in human diabetic nephropathy: sglt2 protein inhibition decreases renal lipid accumulation, inflammation, and the development of nephropathy in diabetic mice. J Biol Chem. 2017;292(13):5335–48. https://doi.org/10.1074/jbc.m117.779520.
10. Rahmoune H, Thompson PW, Ward JM, Smith CD, Hong G, Brown J. Glucose transporters in human renal proximal tubular cells isolated from the urine of patients with non-insulin-dependent diabetes. Diabetes. 2005;54(12):3427–34. https://doi.org/10.2337/diabetes.54.12.3427.
11. Abdul-Ghani MA, Norton L, Defronzo RA. Role of sodium-glucose cotransporter 2 (SGLT 2) inhibitors in the treatment of type 2 diabetes. Endocr Rev. 2011;32(4):515–31. https://doi.org/10.1210/er.2010-0029.
12. Wilding JP. The role of the kidneys in glucose homeostasis in type 2 diabetes: clinical implications and therapeutic significance through sodium glucose co-transporter 2 inhibitors. Metabolism. 2014;63(10):1228–37. https://doi.org/10.1016/j.metabol.2014.06.018.
13. Górriz JL, Navarro-González JF, Ortiz A, Vergara A, Nuñez J, Jacobs-Cachá C, Martínez-Castelao A, Soler MJ. Sodium-glucose cotransporter 2 inhibition: towards an indication to treat diabetic kidney disease. Nephrol Dial Transpl. 2020;35(Suppl 1):i13–23. https://doi.org/10.1093/ndt/gfz237.
14. Takata S, Sawa Y, Uchiyama T, Ishikawa H. Expression of toll-like receptor 4 in glomerular endothelial cells under diabetic conditions. Acta Histochem Cytochem. 2013;46(1):35–42. https://doi.org/10.1267/ahc.13002.
15. Sawa Y, Takata S, Hatakeyama Y, Ishikawa H, Tsuruga E. Expression of toll-like receptor 2 in glomerular endothelial cells and promotion of diabetic nephropathy by *Porphyromonas gingivalis* lipopolysaccharide. PLoS ONE. 2014;9(5):e97165. https://doi.org/10.1371/journal.pone.0097165.
16. Kajiwara K, Takata S, To TT, Takara K, Hatakeyama Y, Tamaoki S, Darveau RP, Ishikawa H, Sawa Y. The promotion of nephropathy by *Porphyromonas gingivalis* lipopolysaccharide via toll-like receptors. Diabetol Metab Syndr. 2017;9:73. https://doi.org/10.1186/s13098-017-0271-8.
17. Goulopoulou S, McCarthy CG, Webb RC. Toll-like receptors in the vascular system: sensing the dangers within. Pharmacol Rev. 2016;68(1):142–67. https://doi.org/10.1124/pr.114.010090.
18. Kawai T, Akira S. The role of pattern-recognition receptors in innate immunity: update on toll-like receptors. Nat Immunol. 2010;11(5):373–84. https://doi.org/10.1038/ni.1863.
19. Vijay K. Toll-like receptors in immunity and inflammatory diseases: past, present, and future. Int Immunopharmacol. 2018;59:391–412. https://doi.org/10.1016/j.intimp.2018.03.002.
20. Cheng A, Dong Y, Zhu F, Liu Y, Hou FF, Nie J. AGE-LDL activates toll like receptor 4 pathway and promotes inflammatory cytokines production in renal tubular epithelial cells. Int J Biol Sci. 2013;9(1):94–107. https://doi.org/10.7150/ijbs.5246.
21. Dasu MR, Devaraj S, Zhao L, Hwang DH, Jialal I. High glucose induces toll-like receptor expression in human monocytes: mechanism of activation. Diabetes. 2008;57(11):3090–8. https://doi.org/10.2337/db08-0564.
22. Devaraj S, Tobias P, Kasinath BS, Ramsamooj R, Afify A, Jialal I. Knockout of toll-like receptor-2 attenuates both the proinflammatory state of diabetes and incipient diabetic nephropathy. Arterioscler Thromb Vasc Biol. 2011;31(8):1796–804. https://doi.org/10.1161/atvbaha.111.228924.
23. Li F, Yang N, Zhang L, Tan H, Huang B, Liang Y, Chen M, Yu X. Increased expression of toll-like receptor 2 in rat diabetic nephropathy. Am J Nephrol. 2010;32(2):179–86. https://doi.org/10.1159/000317023.
24. Lin M, Yiu WH, Wu HJ, Chan LY, Leung JC, Au WS, Chan KW, Lai KN, Tang SC. Toll-like receptor 4 promotes tubular inflammation in diabetic nephropathy. J Am Soc Nephrol. 2012;23(1):86–102. https://doi.org/10.1681/asn.2010111210.
25. Mudaliar H, Pollock C, Komala MG, Chadban S, Wu H, Panchapakesan U. The role of toll-like receptor proteins (TLR) 2 and 4 in mediating inflammation in proximal tubules. Am J Physiol Ren Physiol. 2013;305(2):F143–154. https://doi.org/10.1152/ajprenal.00398.2012.
26. Dasu MR, Devaraj S, Park S, Jialal I. Increased toll-like receptor (TLR) activation and TLR ligands in recently diagnosed type 2 diabetic subjects. Diabetes Care. 2010;33(4):861–8. https://doi.org/10.2337/dc09-1799.
27. Jialal I, Major AM, Devaraj S. Global toll-like receptor 4 knockout results in decreased renal inflammation, fibrosis and podocytopathy. J Diabetes Complications. 2014;28(6):755–61. https://doi.org/10.1016/j.jdiacomp.2014.07.003.
28. Kaur H, Chien A, Jialal I. Hyperglycemia induces toll like receptor 4 expression and activity in mouse mesangial cells: relevance to diabetic nephropathy. Am

J Physiol Ren Physiol. 2012;303(8):F1145–1150. https://doi.org/10.1152/ajprenal.00319.2012.
29. Van Beijnum JR, Buurman WA, Griffioen AW. Convergence and amplification of toll-like receptor (TLR) and receptor for advanced glycation end products (RAGE) signaling pathways via high mobility group B1 (HMGB1). Angiogenesis. 2008;11(1):91–9. https://doi.org/10.1007/s10456-008-9093-5.
30. Wong FS, Wen L. Toll-like receptors and diabetes. Ann N Y Acad Sci. 2008;1150:123–32. https://doi.org/10.1196/annals.1447.063.
31. Feng Y, Yang S, Ma Y, Bai XY, Chen X. Role of toll-like receptors in diabetic renal lesions in a miniature pig model. Sci Adv. 2015;1(5):e1400183. https://doi.org/10.1126/sciadv.1400183.
32. Ma J, Chadban SJ, Zhao CY, Chen X, Kwan T, Panchapakesan U, Pollock CA, Wu H. TLR4 activation promotes podocyte injury and interstitial fibrosis in diabetic nephropathy. PLoS ONE. 2014;9(5):e97985. https://doi.org/10.1371/journal.pone.0097985.
33. Kajiwara K, Sawa Y. Overexpression of SGLT2 in the kidney of a *P. gingivalis* LPS-induced diabetic nephropathy mouse model. BMC Nephrol. 2021;22(1):287. https://doi.org/10.1186/s12882-021-02506-8.
34. Kajiwara K, Sawa Y, Fujita T, Tamaoki S. Immunohistochemical study for the expression of leukocyte adhesion molecules, and FGF23 and ACE2 in *P. Gingivalis* LPS-induced diabetic nephropathy. BMC Nephrol. 2021;22(1):3. https://doi.org/10.1186/s12882-020-02203-y.
35. Li G, Sun Y, Huang Y, Lian J, Wu S, Luo D, Gong H. *Fusobacterium nucleatum*-derived small extracellular vesicles facilitate tumor growth and metastasis via TLR4 in breast cancer. BMC Cancer. 2023;23(1):473. https://doi.org/10.1186/s12885-023-10844-z.
36. Kong C, Yan X, Zhu Y, Zhu H, Luo Y, Liu P, Ferrandon S, Kalady MF, Gao R, He J, et al. *Fusobacterium nucleatum* promotes the development of colorectal cancer by activating a cytochrome p450/epoxyoctadecenoic acid axis via TLR4/Keap1/NRF2 signaling. Cancer Res. 2021;81(17):4485–98. https://doi.org/10.1158/0008-5472.can-21-0453.
37. Engevik MA, Danhof HA, Ruan W, Engevik AC, Chang-Graham AL, Engevik KA, Shi Z, Zhao Y, Brand CK, Krystofiak ES, et al. Fusobacterium nucleatum Secretes Outer Membrane Vesicles Promotes Intestinal Inflamm mBio. 2021;12(2). https://doi.org/10.1128/mbio.02706-20.
38. Yang Y, Weng W, Peng J, Hong L, Yang L, Toiyama Y, Gao R, Liu M, Yin M, Pan C, et al. *Fusobacterium nucleatum* increases proliferation of colorectal cancer cells and tumor development in mice by activating toll-like receptor 4 signaling to nuclear factor-κb, and up-regulating expression of microRNA-21. Gastroenterology. 2017;152(4):851–e866824. https://doi.org/10.1053/j.gastro.2016.11.018.
39. Furman BL. Streptozotocin-induced diabetic models in mice and rats. Curr Protoc. 2021;1(4):e78. https://doi.org/10.1002/cpz1.78.
40. Wszola M, Klak M, Kosowska A, Tymicki G, Berman A, Adamiok-Ostrowska A, Olkowska-Truchanowicz J, Uhrynowska-Tyszkiewicz I, Kaminski A. Streptozotocin-induced diabetes in a mouse model (balb/c) is not an effective model for research on transplantation procedures in the treatment of type 1 diabetes. Biomedicines. 2021;9(12). https://doi.org/10.3390/biomedicines9121790.
41. Li Q, Li L, Fei X, Zhang Y, Qi C, Hua S, Gong F, Fang M. Inhibition of autophagy with 3-methyladenine is protective in a lethal model of murine endotoxemia and polymicrobial sepsis. Innate Immun. 2018;24(4):231–9. https://doi.org/10.1177/1753425918771170.
42. Mémain N, Arvaniti K, Bruneel F, Leport C, Wolff M, Regnier B. Septic shock with liver abscess in an immunocompetence patient. Presentation of an unusual Fusobacterium nucleatum infection. Presse Med. 2001;30(36):1777–9.
43. Shao W, Fujiwara N, Mouri Y, Kisoda S, Yoshida K, Yoshida K, Yumoto H, Ozaki K, Ishimaru N, Kudo Y. Conversion from epithelial to partial-EMT phenotype by *Fusobacterium nucleatum* infection promotes invasion of oral cancer cells. Sci Rep. 2021;11(1):14943. https://doi.org/10.1038/s41598-021-94384-1.
44. Koike R, Cueno ME, Nodomi K, Tamura M, Kamio N, Tanaka H, Kotani A, Imai K. Heat-killed *fusobacterium nucleatum* triggers varying heme-related inflammatory and stress responses depending on primary human respiratory epithelial cell type. Molecules. 2020; 25(17). Aug 24;25(17):3839. https://doi.org/10.3390/molecules25173839
45. Shabir K, Gharanei S, Orton S, Patel V, Chauhan P, Karteris E, Randeva HS, Brown JE, Kyrou I. Asprosin exerts pro-inflammatory effects in THP-1 macrophages mediated via the toll-like receptor 4 (tlr4) pathway. Int J Mol Sci. 2022;24(1). https://doi.org/10.3390/ijms24010227.
46. Yang S, Sugawara S, Monodane T, Nishijima M, Adachi Y, Akashi S, Miyake K, Hase S, Takada H. *Micrococcus luteus* teichuronic acids activate human and murine monocytic cells in a CD14- and toll-like receptor 4-dependent manner. Infect Immun. 2001;69(4):2025–30. https://doi.org/10.1128/iai.69.4.2025-2030.2001.
47. Miyazawa M, Ito Y, Kosaka N, Nukada Y, Sakaguchi H, Suzuki H, Nishiyama N. Role of TNF-α and extracellular ATP in THP-1 cell activation following allergen exposure. J Toxicol Sci. 2008;33(1):71–83. https://doi.org/10.2131/jts.33.71.
48. Sawa Y, Ueki T, Hata M, Iwasawa K, Tsuruga E, Kojima H, Ishikawa H, Yoshida S. LPS-induced IL-6, IL-8, VCAM-1, and ICAM-1 expression in human lymphatic endothelium. J Histochem Cytochem. 2008;56(2):97–109. https://doi.org/10.1369/jhc.7a7299.2007.
49. Takenawa T, Kanai T, Kitamura T, Yoshimura Y, Sawa Y, Iida J. Expression and dynamics of podoplanin in cultured osteoblasts with mechanostress and mineralization stimulus. Acta Histochem Cytochem. 2018;51(1):41–52. https://doi.org/10.1267/ahc.17031.
50. Maldonado-Cervantes MI, Galicia OG, Moreno-Jaime B, Zapata-Morales JR, Montoya-Contreras A, Bautista-Perez R, Martinez-Morales F. Autocrine modulation of glucose transporter SGLT2 by IL-6 and TNF-alpha in LLC-PK (1) cells. J Physiol Biochem. 2012;68(3):411–20. https://doi.org/10.1007/s13105-012-0153-3.
51. Kim YK, Hwang JH, Lee HT. Differential susceptibility to lipopolysaccharide affects the activation of toll-like-receptor 4 signaling in THP-1 cells and PMA-differentiated THP-1 cells. Innate Immun. 2022;28(3–4):122–9. https://doi.org/10.1177/17534259221100170.
52. Li M, Khan AM, Maderdrut JL, Simon EE, Batuman V. The effect of PACAP38 on MyD88-mediated signal transduction in ischemia-/hypoxia-induced acute kidney injury. Am J Nephrol. 2010;32(6):522–32. https://doi.org/10.1159/000321491.
53. Ding Y, Yang H, Xiang W, He X, Liao W, Yi Z. CD200R1 agonist attenuates LPS-induced inflammatory response in human renal proximal tubular epithelial cells by regulating TLR4-MyD88-TAK1-mediated NF-κB and MAPK pathway. Biochem Biophys Res Commun. 2015;460(2):287–94. https://doi.org/10.1016/j.bbrc.2015.03.026.
54. Han YW. *Fusobacterium nucleatum*: a commensal-turned pathogen. Curr Opin Microbiol. 2015;23:141–7. https://doi.org/10.1016/j.mib.2014.11.013.
55. Vestri S, Okamoto MM, de Freitas HS, Aparecida Dos Santos R, Nunes MT, Morimatsu M, Heimann JC, Machado UF. Changes in sodium or glucose filtration rate modulate expression of glucose transporters in renal proximal tubular cells of rat. J Membr Biol. 2001;182(2):105–12. https://doi.org/10.1007/s00232-001-0036-y.
56. Tabatabai NM, Sharma M, Blumenthal SS, Petering DH. Enhanced expressions of sodium-glucose cotransporters in the kidneys of diabetic Zucker rats. Diabetes Res Clin Pract. 2009;83(1):e27–30. https://doi.org/10.1016/j.diabres.2008.11.003.
57. Syed MM, Phulwani NK, Kielian T. Tumor necrosis factor-alpha (TNF-α) regulates toll-like receptor 2 (TLR2) expression in microglia. J Neurochem. 2007;103(4):1461–71. https://doi.org/10.1111/j.1471-4159.2007.04838.x.
58. Freitas HS, Anhê GF, Melo KF, Okamoto MM, Oliveira-Souza M, Bordin S, Machado UF. Na(+)-glucose transporter-2 messenger ribonucleic acid expression in kidney of diabetic rats correlates with glycemic levels: involvement of hepatocyte nuclear factor-1alpha expression and activity. Endocrinology. 2008;149(2):717–24.
59. Ghezzi C, Loo DDF, Wright EM. Physiology of renal glucose handling via SGLT1, SGLT2 and GLUT2. Diabetologia. 2018; 61(10):2087–2097. https://doi.org/10.1007/s00125-018-4656-5

Publisher's note